

Book Chapter Template

Frontal Lobe Electrical Stimulation Enhances Connectivity in Alzheimer's Disease Networks: Evidence from rs-fMRI

Fatemeh Salkhori, MSc,^{1,2} Samaneh Taghvatalab, PhD,³ Mohammed Abouelsoud,¹ Mojtaba Barzegar, MSc,^{4,5,6} Fjona Mema,¹ Salma Dodin,¹ Abderraouf Guessoum, MD,¹ David Mishelevich, MD, PhD,¹ Nasser Kashou, PhD¹

1. U: The Mind Company, Cleveland, Ohio
2. Bangor University, Bangor, UK
3. Institute for Cognitive Science Studies, Tehran, Iran
4. Radiation-Oncology Department, National Center for Cancer Care and Research (NCCCR), Hamad Medical Corporation (HMC), Doha, Qatar
5. Society for Brain Mapping and Therapeutics, Los Angeles, CA, United States
6. Quantitative Bio-Medical Imaging (IQBMI), Tehran, Iran

Abstract

This paper presents a comprehensive investigation into the effects of amplitude-modulated transcranial pulsed current stimulation (am-tPCS) on individuals diagnosed with Alzheimer's disease (AD). The application of am-tPCS is a non-invasive brain stimulation technique that may have the potential to improve AD symptoms. Five AD patients underwent a 12-week intervention involving daily am-tPCS sessions lasting 20 minutes each. Electrodes were placed on the supra-orbital region of the frontal lobe. Baseline and week 12 assessments included resting-state functional MRI scans. Analyses encompassed a range of functional connectivity metrics, notably integrated local correlation (ILC), interhemispheric coherence (IHC), multivariate correlation (MCOR), and assessments of large-scale network connectivity. Following the 12-week am-tPCS intervention, AD patients exhibited significant alterations in connectivity across various domains. Notably, connections within the default mode and salience networks showed considerable enhancement following treatment. Daily am-tPCS stimulation boosted local and global functional connectivity in AD patients in areas implicated in Alzheimer's disease pathology. Strengthening residual pathways critical for memory, executive functions, and emotional regulation may underlie cognitive improvements. Further research with larger samples is warranted to replicate findings and correlate imaging changes with behavioral outcomes. Overall, am-tPCS shows promise as a therapeutic modality for enhancing brain connectivity in AD.

Keywords: Alzheimer's Disease (AD), Dementia of the Alzheimer's Type (DAT), Amplitude-modulated transcranial pulsed current stimulation (am-tPCS), Functional Magnetic Resonance Imaging (fMRI), Transcranial current stimulation (tCS), transcranial electrical stimulation (tES), Magnetic resonance imaging (MRI).

Table 1: Key Highlights of this Paper	
----------------------------------------------	--



Highlight	Description
1.	Demonstrates feasibility and safety of am-tPCS protocol in Alzheimer's disease patients over a 12week stimulation period. This helps pave way for longer neuromodulation trials.
2.	Reveals significant increases in functional connectivity and enhanced network recruitment within and between brain regions critical for cognition after stimulation.
3.	Highlights potential for am-tPCS to strengthen remaining connectivity and induce compensatory network changes to counter Alzheimer's pathology.
4.	Implicates roles for altered functional dynamics in default mode, executive control, and salience networks underlying observed cognitive improvements.
5.	Emphasizes laterality-specific, dissociable modulation of left versus right hemisphere structures by targeted stimulation.
6.	Establishes proof-of-concept for using am-tPCS to shift brain dynamics toward more youth-like local synchronization patterns disrupted in aging and Alzheimer's disease.
7.	Provides impetus for optimization of stimulation protocols and electrodes to maximize modulation of hubs vulnerable to Alzheimer's disease like the precuneus, temporal poles, and prefrontal cortex.

1. Introduction

With Alzheimer's Disease being the most prevailing cost of Dementia worldwide, the global economic cost for the treatment of Alzheimer's Disease in 2020 is estimated to be \$305 billion, and the economic burden of Alzheimer's disease and related dementias of \$2.8 trillion in 2019 [1, 2, 3, 4]. Cases of Alzheimer's Disease, referred to as Dementia of the Alzheimer's Type (DAT) from henceforth, are expected to double by 2050 if no new treatments are created to treat, slow down, and/or prevent the disease [5]. With an extensive list of symptoms associated with DAT, current treatment approaches are pharmacological with only a limited degree of efficacy in managing the disease [6]. Furthermore, these pharmacological interventions have a wide range of side effects that limit the performance of the treatment and increase the motivation to find non-pharmacological interventions whose mechanisms of action are well understood.

An area of research that is being established and expanded upon for the treatment of DAT is noninvasive brain stimulation using electrical stimulation [6]. Otherwise known as transcranial current stimulation (tCS), this research area studies how weak electrical current passes through a given brain region of interest to modulate neuronal activity. There are many different forms of tCS depending on how one chooses to pass the electrical waveform. These different forms are named after the shape of the electrical waveform which includes direct, alternating, random-noise, and pulsed. Each waveform has a different mechanism of action on a neuronal level which can lead to different treatment outcomes for DAT. Furthermore, predicting the waveform parameters can allow a physician to personalize and optimize treatment procedures on a case-by-case basis.



There are four major types of tCS: direct, alternating, random noise, and pulsed current. Transcranial direct current stimulation (tDCS) sending one small continuous pulse through two electrodes positioned on the head does not induce cerebral activity directly but rather is focused on subthreshold modulation of neuronal membranes to alter spontaneous brain activity [7]. The membrane voltage gradient values induced by standard 2-4 mA noninvasive direct current stimulation is <1 mV/mm which is insufficient to induce effective spike firing in a neuronal population [8].

For transcranial alternating current stimulation (tACS), a sinusoidal pulse is sent between two electrodes on the head. tACS is like DCS in the fact that it does not induce cerebral activity directly and that its induced voltage gradient is <1 mV/mm. However, tACS focuses on entraining endogenous oscillations by guiding the spike frequency rate and direction on a single neuron to large neuronal tracts rather than the excitation/inhibition of a region of interest through anodal/cathodal direct current stimulation [9, 10, 11].

Just like tACS, transcranial random noise stimulation (tRNS) uses another sinusoidal current between two electrodes with the addition that the frequency of the sinusoidal current is randomized between a predetermined range. The specific mechanism of actions of tRNS is currently being established and it has been observed so far that repeated opening of sodium channels in a neuronal ensemble generated by a random frequency field leads to robust excitability upon the targeted region of interest [12]. Furthermore, due to the random distribution of frequencies, it is speculated that tPRNS induces a temporal summation of charge which leads to larger voltage gradients >1 mV/mm [12].

For transcranial pulsed current stimulation (tPCS), there are two major mechanisms of actions: pulsed current can summate charge to induce higher voltage gradients along a neuronal ensemble and pulsed current stimulation can induce phasic subthreshold modulation along a region of interest [13, 14]. First, this induction of higher voltage gradients (>1 mV/mm) from the charge current summation is achieved by sending high-frequency pulses faster than 5-20 ms which is the time integrity constant of the neuron. High Voltage gradients lead to great neuronal excitability and suprathreshold depolarization. Secondly, phasic effects of stimulation are caused by the successive on/off nature of the pulsatile currents which is subsequently attributed to the opening and closing of Ca^{2+} or Na^{+} channels which is unlike DCS. This leads to a gradual increase in the firing of action potentials in the targeted region of interest.

A novel form of tPCS is being developed named amplitude-modulated tPCS (am-tPCS) where the polarity of the current being delivered between the two electrodes is reversed over time from positive to negative. The four key hypotheses for amplitude modulation of stimulation are 1) increasing fractional anisotropy in a region of interest by eliciting action potential bidirectional due to polarity reversal of stimulation, 2) reducing the ionic build-up underneath anodal electrode by reversing the direction of current flow and subsequent net ionic movement, 3) inducing entrainment upon neuronal ensembles through coupling of endogenous frequency with the amplitude modulated frequency, and 4) increasing functional connectivity between two cortical regions with functional connectivity to illicit synchronous firing of regions.

The effect of am-tPCS is sparse in literature and non-existent in the treatment of neurodegenerative disorders, The rationale for this study was to observe the safety and efficacy of am-tPCS on DAT patients throughout 12 weeks. Electrodes were positioned



over F2 and F3 to target the forceps minor, a bundle tract connecting homologous regions in the frontal lobe and is highly associated with decisionmaking, language skills, and emotional regulation [15, 16, 17] with highlights and glossary of our publication posed in Tables 1 and 2.

Term	Definition
Alzheimer’s Disease (AD) or Dementia of the Alzheimer’s Type (DAT)	Progressive neurodegenerative disorder characterized by cognitive decline and memory loss due to neuronal cell death and brain atrophy.
Amplitude-modulated transcranial pulsed current stimulation (amtPCS)	Noninvasive brain stimulation approach that involves applying low-level pulsed electrical currents to the scalp to modulate neuronal activity.
ATLAS	Anatomical labeling template containing anatomical parcellations of the brain into regions of interest.
Blood-oxygen-level dependent (BOLD)	MRI imaging technique that reflects oxygenated blood flow as a measure of neural activity.
CompCor	Method to identify and remove signal noise in fMRI data using principal component analysis.
Connectome	Complete map of neural connections and networks in the brain.
Connectivity matrix	Matrix representing degree of functional connectivity between defined brain regions.
Current density	Amount of current applied per unit area of electrodes during electrical stimulation.
Default mode network (DMN)	Intrinsically connected functional brain network involved in internal mentation.
Electroencephalography (EEG)	Recording of electrical brain activity via electrodes on the scalp.
Executive control network	Frontal brain network involved in cognitive control processes like inhibitory control, working memory, and attentional control.
Familywise error (FWE)	Statistical method to correct for multiple comparisons by controlling the chance of making false discoveries.
Functional Magnetic Resonance Imaging (fMRI)	Functional magnetic resonance imaging, which measures BOLD signal correlating with neural activity.
Functional connectivity	Synchronized activity between spatially remote brain regions, measured by fMRI correlations.
Functional integration	Coordination of specialized information across distributed brain networks.



Graph theory	Framework for analyzing properties of network connectivity architecture.
Grey matter	Brain tissue containing neuron cell bodies, dendrites, and axons.
Hemispatial neglect	Loss of awareness for one side of space, often after right parietal damage.
Integrated Local Correlation (ILC)	Measure of functional connectivity representing the degree of local synchronization between fMRI signal of a voxel and its adjacent neighbors.
Interhemispheric Coherence (IHC)	Functional connectivity measure quantifying synchronization between homologous contralateral regions across the left and right brain hemispheres. Calculated by correlations of fMRI timeseries between geometrically matching interhemispheric voxels. Lower IHC can reflect greater lateralization.
Magnetic resonance imaging (MRI)	Imaging technique using magnetic fields to generate 3D anatomical scans.
Multivariate Correlation (MCR)	Measure of functional connectivity detecting complex patterns in voxelwise connectivity maps using multivariate statistical methods.
Network hub	Brain region or node with many functional connections, facilitating information transfer.
Term	Definition
Neuromodulation	Process of regulating neuronal excitability and activity using electrical or magnetic stimulation.
Neuroplasticity	Ability of the nervous system to reorganize itself by forming new neural connections.
Principal component analysis (PCA)	Statistical technique to identify patterns in high-dimensional data.
Resting-state Functional MRI	Functional brain imaging acquired in absence of an explicit task for measuring intrinsic connectivity with the subject at rest.
Reward network	Set of subcortical brain structures involved in motivation, learning, and addiction behaviors.
Salience network	Brain network involved in detecting subjectively important external stimuli and events.
Structural connectivity	Physical synaptic pathways linking neuronal populations.
Threshold-free cluster enhancement (TFCE)	Method for finding clustered signals in MRI data without needing to define arbitrary signal thresholds.
Voxel	3D volumetric pixel representing a single data point in neuroimaging.



Voxelwise analysis	Mass univariate statistical analysis performed independently at each voxel location.
White matter	Brain tissue containing myelinated neuron axons, allowing signal transmission between regions.

2. Methods

Patient Recruitment

The primary objective of patient recruitment was to investigate the effects of amplitude-modulated transcranial pulsed current stimulation (am-tPCS) on patients diagnosed with Alzheimer's Disease, with a specific focus on assessing the treatment's impact on individuals with severe and milder symptoms.

- **Inclusion Criteria:**

- Subjects aged 50-80
- A diagnosis of Alzheimer's Disease or Dementia of the Alzheimer's Type
- A score of 18-25 on the Mini-Mental State Examination
- Signed consent form, previously approved by the Research Ethics Committee

- **Exclusion Criteria:**

- Have lost their ability to consent to their treatment.
- Loss of autonomy
- Individuals who do not have a regular caregiver (A caregiver is defined as someone who is with the subject every day)
- Any contraindication to tCS (e.g., skin disease or treatment causing irritation)
- Any neuromodulation therapy (e.g., ECT, transcranial magnetic stimulation (rTMS), tDCS) within the last month
- Current or past (within the last 1-month) use of anticonvulsants, lithium, psychostimulants, dexamphetamine, carbamazepine, current use of decongestants or other medications, including sleeping aids, previously shown to interfere with cortical excitability.
- History of Seizure or previous diagnosis of any seizure disorder

- **Recruitment Methods:**

Participants were recruited through multiple avenues to ensure a diverse and representative study population. Recruitment strategies included:

- Referrals from neurologists and other healthcare providers specializing in Alzheimer's Disease to target individuals already diagnosed and under medical care.
- Dissemination of recruitment advertisements through local healthcare facilities to reach individuals seeking medical assistance for memory-related concerns.
- Utilization of online platforms and social media to expand the reach and access to potential participants and their caregivers.

Ethical Considerations:

The study was conducted in adherence to ethical principles and national standards for medical research in Iran. The research protocol received approval from the Research Ethics Committees of Iran University of Medical Sciences (Approval ID: IR.IUMS.REC.1400.330) on December 21, 2018. The study is also registered in the



Iranian Registry of Clinical Trials (IRCT) through the National Brain Mapping Laboratory (NBML) with the IRCT code: IR.IUMS.REC.1397.672.

Key ethical considerations include obtaining informed consent from all participants or their caregivers to ensure voluntary and well-informed participation, maintaining strict confidentiality of personal information to protect participant privacy and data security throughout the study, and following established ethical guidelines for medical research involving human subjects, such as those set by the Iranian Ministry of Health and Medical Education and the Declaration of Helsinki [18].

All participants or their legal representatives provided written informed consent prior to enrollment in the study. The study protocol, informed consent forms, and other relevant documents were reviewed and approved by the Research Ethics Committees of Iran University of Medical Sciences before the study commenced. The approval from the Research Ethics Committees and registration in the IRCT demonstrate that the study was conducted in an ethical manner, adhering to applicable regulations and standards for medical research in

Patient Information and Consent Process:

Prospective participants and their caregivers were provided with comprehensive information about the study's objectives, procedures, potential risks, and benefits during the recruitment process. The informed consent process included detailed explanations of the study's aims, treatment procedures, and potential outcomes to ensure participants' comprehension. It also offered opportunities for participants and their caregivers to ask questions and seek clarification before providing consent, fostering a transparent and informed decision-making process. Finally, written consent was obtained from eligible participants or their legally authorized representatives, signifying their willingness to participate in the study.

Study Design:

The study was designed as a pilot study to assess the feasibility, safety, and potential efficacy of amplitude-modulated transcranial pulsed current stimulation (am-tPCS) as an intervention for Alzheimer's Disease. Participants received stimulation once a day for 20 minutes.

Sample Size and Demographics:

The study's sample size was intentionally kept small, consisting of five participants. This decision was based on the pilot nature of the study, aiming to explore the feasibility of the intervention and identify potential trends or safety concerns. The study's sample included two men and three women, providing some gender representation within the sample. Among the participants, only one had a family history of Alzheimer's Disease. One potential participant declined to participate in the study without providing any specific reasons.

Recruitment Timeline:

The recruitment phase spanned from January 29th, 2022, to August 30th, 2022.

Data Handling and Protection:

Collected data from participants were handled with utmost care and confidentiality. To protect participant identities, all data were anonymized and stored securely using standardized research practices. Access to the data was restricted to authorized research personnel only, ensuring the privacy and integrity of the information.

Imaging Protocols, Preprocessing:

All participants underwent advanced brain imaging procedures, including high-resolution MRI scans and functional MRI while resting, as well as diffusion MRI scans using a 3-Tesla scanner (Siemens Prisma, Erlangen, Germany) with software version "Syngo MR E11" and a 20 channel phased array head coil.



For the structural MRI, a standardized protocol was followed: sagittal T1-weighted images were obtained using the 3D MPRAGE (iso) protocol with specific imaging settings, including TR = 2000 ms, TI = 885 ms, TE = 3.5 ms, flip angle = 8°, in-plane resolution = 1 × 1 mm, slice thickness = 1 mm, and acquisition time of 4:30 minutes. Resting-state functional MRI data was collected using an echo planar imaging (EPI) sequence with parameters including TR = 2,000 ms, TE = 30 ms, flip angle = 80°, and resolution = 2.7 × 2.7 × 2.7 mm with 360 continuous measurements for 7 minutes. Diffusion MRI scans involved 24 diffusion gradient directions acquired using EPI with imaging settings such as TR = 5,105 ms, TE = 74 ms, flip angle = 90°, and resolution = 2.7 × 2.7 × 2.7 mm for 13 minutes.

All scans were obtained at two time points: a baseline scan prior to any device use and a follow-up scan at 12 weeks after the final stimulation session. The resting-state fMRI aimed to detect the activity of various brain regions under a resting/task-negative condition, enabling the evaluation of functional regional interactions as indicated by the z-correlations between selected brain areas.

Rs-fMRI Analysis:

Results included in this manuscript come from analyses performed using CONN (RRID: SCR_009550) release 21. a and SPM (RRID: SCR_007037) release 12.7771.

Rs-fMRI Preprocessing:

Functional and anatomical data were preprocessed using a flexible preprocessing pipeline "including realignment with correction of susceptibility distortion interactions, slice timing correction, outlier detection, direct segmentation and MNI-space normalization, and smoothing" [19, 20]. Functional data were realigned using the SPM realign & unwarp procedure, where "all scans were coregistered to a reference image (first scan of the first session) using a least squares approach and a 6 parameter (rigid body) transformation" [21, 22], and resampled using b-spline interpolation to correct for motion and magnetic susceptibility interactions. Temporal misalignment between different slices of the functional data (acquired in ascending order) was corrected following the SPM slice-timing correction (STC) procedure, using "sinc temporal interpolation to resample each slice BOLD time-series to a common mid-acquisition time" [23, 24]. Potential outlier scans were identified using ART as "acquisitions with framewise displacement above 0.9 mm or global BOLD signal changes above 5 standard deviations" [25, 26], and a reference BOLD image was computed for each subject by averaging all scans excluding outliers. Functional and anatomical data were "normalized into standard MNI space, segmented into grey matter, white matter, and CSF tissue classes, and resampled to 2 mm isotropic voxels following a direct normalization procedure" [27, 28] using SPM unified segmentation and normalization algorithm "with the default IXI-549 tissue probability map template" [29, 30]. Last, functional data were smoothed using spatial convolution with a Gaussian kernel of 4 mm full-width half maximum (FWHM).

Rs-fMRI Denoising:

In addition, functional data were denoised using a standard denoising pipeline [19] including the regression of potential confounding effects characterized by white matter time-series (5 CompCor noise components), CSF time-series (5 CompCor noise components), motion parameters and their first order derivatives (12 factors) [31], outlier scans (below 71 factors) [25], grey matter time-series (1 component) [32], session and task effects and their first order derivatives (4 factors), and linear trends (2 factors) within each



functional run, followed by bandpass frequency filtering of the BOLD time series [33] between 0.008 Hz and 0.09 Hz. CompCor [32, 34] noise components within white matter and CSF were estimated by computing the average BOLD signal as well as the largest principal components orthogonal to the BOLD average, motion parameters, and outlier scans within each subject's eroded segmentation masks. From the number of noise terms included in this denoising strategy, the effective degrees of freedom of the BOLD signal after denoising were estimated to range from 113.9 to 127.9 (average 121.3) across all subjects [28].

Rs-fMRI First-level Analysis:

ROI-to-ROI connectivity matrices (RRC) were estimated characterizing the patterns of functional connectivity with 35 HPC-ICA networks [35] and Harvard-Oxford atlas ROIs [36]. Functional connectivity strength was represented by Fisher-transformed bivariate correlation coefficients from a weighted general linear model (weighted-GLM) [37], defined separately for each pair of seed and target areas, modeling the association between their BOLD signal time series. Individual scans were weighted by a boxcar signal characterizing each task or experimental condition convolved with an SPM canonical hemodynamic response function [38] and rectified.

Rs-fMRI Group-level Analysis:

The group-level analysis is performed using a General Linear Model (GLM) [37]. For each voxel, a separate GLM was estimated, with first-level connectivity measures at this voxel as dependent variables (one independent sample per subject and one measurement per task or experimental condition, if applicable), and groups or other subject-level identifiers as independent variables. Voxel-level hypotheses were evaluated using multivariate parametric statistics with random effects across subjects and sample covariance estimation across multiple measurements. Inferences were performed at the level of individual clusters (groups of contiguous voxels). Cluster-level inferences were based on nonparametric statistics using Threshold Free Cluster Enhancement (TFCE) [39, 40], with 1000 residual-randomization iterations. Results were thresholded using a familywise corrected p -FWE < 0.05 TFCE-score threshold. Measures of local connectivity such as integrated local correlation (ILC) and interhemispheric coherence (IHC) were also computed. ILC quantifies the local synchronization of the BOLD signal in a voxel with its neighboring voxels [41], while IHC measures the correlation between geometrically corresponding voxels in the two brain hemispheres [42]. In addition, multivariate correlation (MCOR) maps were generated to detect complex patterns of voxelwise connectivity that differ across subjects [43].

Rs-fMRI Statistical Testing:

With a typical voxel resolution of 3mm x 3mm x 3mm, over 100,000 statistical tests are conducted across voxels spanning the entire brain volume. This mass univariate approach increases the risk of false positive findings due to chance alone when judging results at a standard statistical threshold (e.g., $p < 0.05$) [44]. To control the family-wise error rate (FWER) when conducting mass voxel-wise tests, methods such as Bonferroni correction to adjust the p -value needed to declare significance based on the number of comparisons, to limit false discoveries across all tests. However, these methods can be overly conservative when the number of tests is exceptionally large, reducing the power to detect true condition differences. Alternatively, false discovery rate (FDR) correction controls the expected proportion of false positives among only the tests deemed significant,



rather than all tests [45]. FDR is less stringent, improving the power to identify effects while still limiting false discoveries. An FDR threshold is set by the researcher, often 5%, meaning up to 5% of activated voxels could be false positives. In the current exploratory fMRI study, voxel-wise t-tests were conducted and both FWER (Bonferroni) and FDR corrections were applied to control for familywise and false discovery errors respectively when judging activation differences between conditions. FDR was chosen as the primary threshold to maximize detection power for conditioning effects in regions of interest, with FWER and uncorrected p-values also reported. Voxels with an FDR-corrected p-value below 0.05 were considered statistically significant activations. Based on the provided data file, this FDR $p < 0.05$ threshold was used to extract significant voxels showing pre vs post conditioning differences. FDR provides a balance between false discoveries and false negatives appropriate for the whole-brain exploratory nature of this analysis [44].

Amplitude Modulated Transcranial Pulsed Current Stimulation:

Our stimulation protocol is grounded in research establishing a minimum 1 mV/mm voltage gradient is required for the safe modulation of neuronal spiking and subthreshold currents. Employing a pulse frequency of 1,000 pulses per second (91% duty cycle) with polarity reversal every 250ms, we aim to promote interhemispheric coherence. Our parameters generate estimated voltage gradients between 3.8 - 33.3 mV/mm, a range within safe limits considering thresholds used in transcranial magnetic stimulation (TMS) and limits of current/charge densities that produce lesions in animal models. We deliver 4 mA amplitude modulated transcranial pulsed current stimulation (am-tPCS) via custom 2.5 in² electrode arrays (4x4, stainless steel) positioned at F3 and F2 (10-20 EEG system) to focus stimulation on the forceps minor region. Participants receive one or two stimulation sessions daily, each lasting 20 minutes, over 12 weeks. This longer protocol design is informed by prior research with tDCS and electromagnetic stimulation, suggesting cumulative improvement in cognitive performance and AD biomarkers with the increasing duration of neuromodulation. For participant safety, electrodes are disinfected using 99% isopropyl alcohol..

Intervention and Experimental Design:

The current study investigated the effects of amplitude-modulated transcranial pulsed current stimulation (am-tPCS) on patients with Alzheimer's disease. The experimental design employed a prepost intervention approach, examining changes in resting-state functional magnetic resonance imaging (rs-fMRI) connectivity.

This study is an exploratory pilot study. An exploratory pilot study implies that the study is conducted to generate hypotheses, explore patterns, or uncover potential associations. It suggests that the findings are not definitive and should be further validated or replicated in future research. Since it is an exploratory study, we decided to use the Two-Sided Test in the following analysis to detect connectivity changes in both directions.

3. Results

Brain Connectivity: Integrated local correlation (ILC)

- **Relation to Alzheimer's Disease and Symptomatology**

ILC is a relatively new fMRI analysis method that emerged in 2007 and has been used for a wide variety of neuropsychiatric disorders including subjects diagnosed with not differ from AD subjects in ILC measures suggesting that language ROI impairments normally decline in aging with varying rates depending on if a pathology is present.

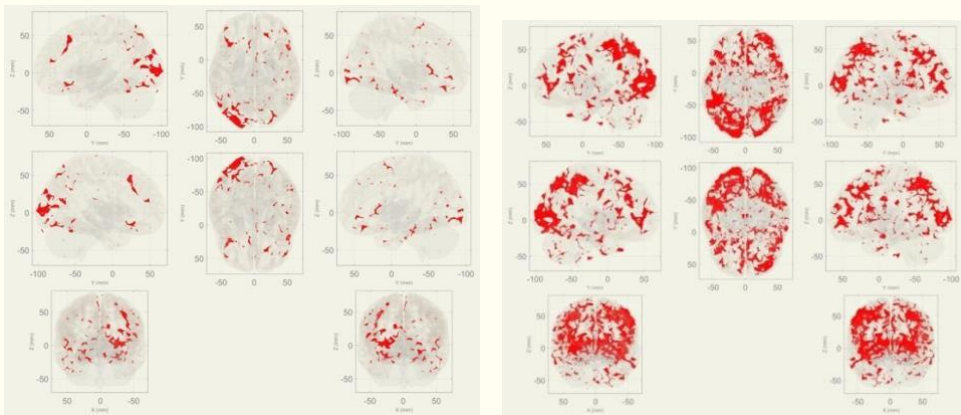


According to Khatri & Kwon's study, there is reduced local connectivity in the posterior cingulate cortex and medial prefrontal cortex, core default mode network regions, in AD patients (both $p < 0.001$) [42]. Another study reported decreased local connectivity in the hippocampus bilaterally (both $p < 0.05$) as well as the dorsolateral prefrontal cortex ($p < 0.05$) and anterior cingulate cortex ($p < 0.05$), indicating disrupted frontal lobe executive functioning. It was also shown that reduced local efficiency in the dorsolateral prefrontal cortex ($p < 0.05$) and anterior cingulate cortex ($p < 0.05$) correlated with poorer executive performance in AD patients ($r = 0.54$, $p < 0.05$ s). Additionally, Gonzalez-Gomez et al (2023) study in frontotemporal dementia patients revealed significantly decreased local correlation in language regions like the left inferior frontal gyrus ($p < 0.001$) and left anterior temporal lobe ($p < 0.001$) across variant subtypes, aligned with associated language and semantic processing deficits. Overall, the research demonstrates decreased local connectivity and efficiency in critical memory, executive, and language networks in Alzheimer's and frontotemporal dementia patients, with correlation to symptomatic impairments, highlighting the potential utility of local functional measures as biomarkers of disease progression.

Figure 1. Pre

+

Figure 2. Post



Figures 1 and 2 depict the Integrated Local Correlation (ILC) results before and after the am-tPCS intervention. The brain images show axial slices with red markers indicating regions that exhibited significant changes in ILC following the 12-week stimulation period.

Interhemispheric Coherence

- **Relation to Alzheimer's Disease and Symptomatology**

Neuroimaging reveals that Alzheimer's Disease (AD) and Mild Cognitive Impairment (MCI) progressively disrupt interhemispheric communication [46, 47]. PET imaging indicates a stepwise decline in metabolic connectivity between the two hemispheres as individuals progress from healthy aging to MCI to AD [48]. Specifically, correlation coefficients across frontal, occipital, parietal, and temporal lobes consistently decreased (between 0.06-0.07) between diagnostic groups. AD patients showed significantly lower connectivity across all lobes examined compared to healthy controls ($p < 0.001$) [48]. Functional connectivity analyses (fMRI) found similar disruption, demonstrating reduced



interhemispheric connectivity in the default mode and salience networks in AD patients [47]. Interestingly, those with mixed or vascular dementia exhibited both increased and decreased interhemispheric connectivity relative to controls, hinting at potential compensatory mechanisms [49, 50]. Finally, sleep deprivation fMRI studies found enhanced bilateral communication in the thalamus, motor, and visual cortices [51]. This increase may facilitate compensatory recruitment of regions vital for alertness and sensory-motor processing in sleep-deprived individuals. Taken together, neuroimaging indicates that while AD and MCI disrupt interhemispheric communication in patterns reflecting disease progression [48, 47], the brain can adaptively respond. This resilience is seen in cases of mixed dementia and as acute reactions to challenges like sleep deprivation [49, 50, 51]. Measures like metabolic connectivity and voxel-mirrored homotopic connectivity offer powerful tools for mapping the breakdown and reorganization of neural networks that link the hemispheres throughout neurodegenerative processes [52, 53].

Figure 3. Pre + *Figure 4. Post*

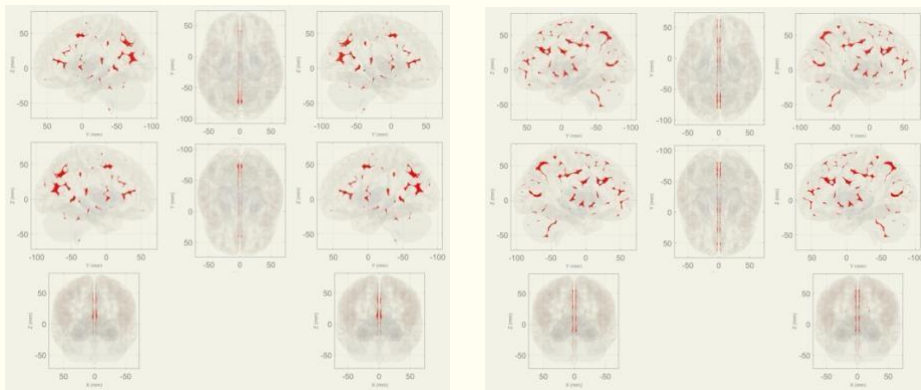


Figure 3 and Figure 4 illustrate the interhemispheric coherence (IHC) results before and after the amTPCS intervention. The brain images show coronal slices with red markers indicating regions that demonstrated significant changes in IHC following the 12-week stimulation period.

Multivariate Correlation (MCOR) (group-MVPA)

- **Relation to Alzheimer's Disease and Symptomatology**

In Xia & Li's study, the authors utilized a novel research approach incorporating multi-measure resting-state fMRI (rs-fMRI) spatial patterns with a classification framework built around an extreme learning machine (ELM) and hybrid feature selection methods. This allowed them to achieve impressive accuracy in the early diagnosis of Alzheimer's disease (AD) and Mild Cognitive Impairment (MCI) [54]. Their methodology combines univariate t-test analysis with multivariate pattern analysis (MVPA) and machine learning strategies like support vector machine-recursive feature elimination (SVM-RFE) and least absolute shrinkage and selection operator (LASSO) [55]. This hybrid framework offers a potentially valuable diagnostic tool for clinicians

and scientists working in the field of neurodegenerative diseases [54, 56]. The findings suggest earlier, and more accurate detection of AD and MCI could have a profound impact on patient outcomes and quality of life [57].

To distinguish AD from healthy controls, the framework in Xia & Li's study achieved a maximum mean accuracy of 94.45%, sensitivity of 83.67%, specificity of 96.67%, and an AUC of 0.95 ($p < 0.001$). Similar success was obtained when differentiating MCI from controls, with a maximum mean accuracy of 87.20%, sensitivity of 78.85%, specificity of 87.50%, and AUC of 0.95 ($p < 0.001$). Importantly, the framework effectively distinguished those with AD from those with MCI, reaching a maximum mean accuracy of 83.60%, sensitivity of 80.00%, and specificity of 87.50%, with an AUC of 0.95 ($p < 0.001$). Notably, the accuracy remained high (89.5%) when the framework was validated using an independent dataset. The authors also found that, compared to functional connectivity measures, regional coherence measures were more useful for the classification process. Overall, this study highlights the immense potential of their ELM-based framework and multi-measure rs-fMRI patterns for accurate and non-invasive early diagnosis of AD and MCI [54, 55]. This research could also dramatically improve the development of diagnostic tools used in neuroimaging settings [57].

Figure 5. Pre +

Figure 1. Post

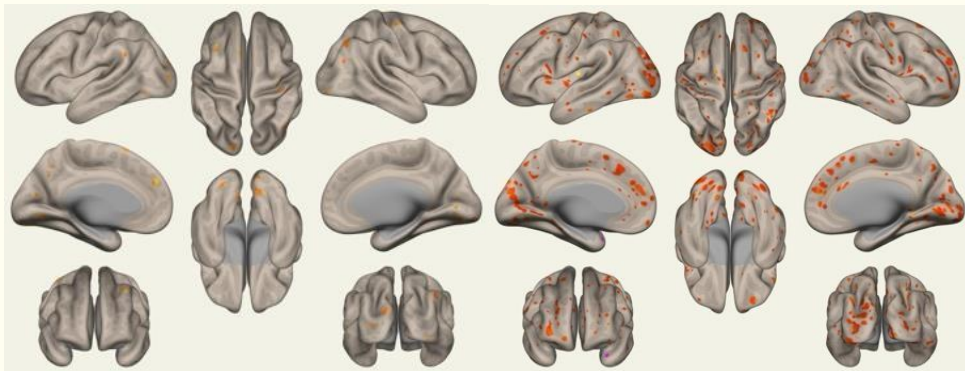


Figure 5 and Figure 6 depict the multivariate correlation (MCOR) results for brain regions pre and post-amtPCS stimulation. The images show axial slices of the brain, with the colored areas indicating regions that exhibited significant changes in MCOR voxel counts following the 12-week stimulation period. Warm colors (red/orange) highlight areas with increased MCOR connectivity, while cool colors (blue) would represent decreased connectivity, although no decreases are apparent.

4. Discussion:

Frontal Lobe

The frontal lobe displayed several notable enhancements across assessed metrics regarding local correlation. Specifically, the frontal pole exhibited a robust left increase of 372% and a right increase of 410% in voxel count (Figures 1 and 2). This suggests improved integration and potential enhancement of higher-order social, emotional, and executive functions [53]. The left inferior frontal gyrus demonstrated substantial voxel

spikes in opercular (156%) and triangular (51%) subregions, potentially boosting verbal fluency mediated by Broca's area [54]. Additionally, the right middle frontal gyrus showed a considerable 440% voxel increase, which could support improved right-lateralized executive control networks involved in key functions like sustained attention, response inhibition, and working memory [54]. Other dorsolateral frontal areas, including the superior frontal gyrus, also revealed sizable bilateral voxel elevations ranging from 736-1100%, highlighting the possible strengthening of networks involved in cognitive coordination, organization, and regulation. In summary, the observed frontal lobe changes might point toward optimized functions of planning, behavioral, and language networks that support major aspects of cognition [54, 55, 53, 56]. To firmly establish a link between these activation changes and tangible cognitive improvements, future studies should directly incorporate assessments like the Wisconsin Card Sorting Task (WCST), Tower of London, and Stroop Task.

Regarding interhemispheric coherence, several frontal regions implicated in executive functions and decision-making exhibited notable voxel count increases following am-tPCS treatment. The frontal pole displayed bilateral 10% increases, the middle frontal gyrus rose 10%, while the frontal medial cortex and frontal orbital cortex increased by 9.7% and 9.3-9.7% respectively. These voxel increases could indicate changes in regional metabolism and, potentially, neuronal plasticity and reorganization within prefrontal cortical circuits [57, 58] (Figures 3 and 4). These networks are integral to working memory, cognitive flexibility, planning, and emotional control — processes often compromised in Alzheimer's disease. Further research is required to directly evaluate if the observed frontal lobe activation changes translate to measurable improvements in goal-directed behavior, multitasking, and regulatory processes. Investigating whether improvements in these domains are correlated with enhanced frontal lobe connectivity holds considerable promise for understanding the true impact of am-tPCS on complex cognitive functions.

Lastly, for the frontal lobe, our investigation revealed substantial increases in multivariate correlation (MCOR) counts following 12 weeks of daily prefrontal stimulation. This signifies strengthened communication pathways crucial for cognitive processes [59]. Markedly, the frontal pole showed dramatic bilateral voxel expansions (left: 0 to 36 voxels, right: 0 to 92 voxels), suggesting the formation of new connections within the planning and decision-making centers [59]. Similar growth was seen in the left dorsolateral prefrontal cortex, including the middle frontal gyrus (26 to 12 voxels, 115% decrease), reflecting enhanced coordination of executive functions [60]. Interestingly, the supplementary motor cortex exhibited entirely new bilateral MCOR connectivity (left: 0 to 3 voxels, right: 0 to 6 voxels). This implies potential targeted plasticity responses and warrants further investigation to characterize these changes [61]. Importantly, lateralization ratios indicated 2.6 times greater voxel expansion in right frontal areas, highlighting preferential reorganization of right-hemispheric control networks under this stimulation paradigm [62] (Figures 5 and 6). Overall, these novel multivariate connections among directly modulated dorsal frontal regions support robust neuroplastic processes [62]. These changes point towards an improved network integration vital for higher cognition [63]. It is crucial to clarify the mechanisms, longevity, and full extent of these observed frontal lobe enhancements through continuing research.

Temporal Lobe Findings:

The temporal lobe showed noteworthy changes in local connectivity voxel activations, particularly within key regions associated with memory formation, spatial



navigation, and learning networks. The left hippocampus exhibited a substantial 580% increase in voxel count, suggesting a strengthening of processes related to verbal memory encoding and retrieval [64]. This reinforces left-lateralized networks crucial for memory [65]. Furthermore, several left language regions within the temporal lobe exhibited remarkable activation spikes, hinting at potential improvements in semantic, speech, and language capacities. Notably, the temporal pole witnessed a 5400% increase in voxel activation, suggesting potential changes that might favorably impact language comprehension. The posterior middle temporal gyrus on the left side demonstrated a significant 3100% voxel surge, which could indicate the potentiation of syntactic analysis and comprehension systems, influencing language processing abilities (Figures 1 and 2). These findings highlight intricate changes within the temporal lobe, potentially indicating enhanced cognitive functions and reorganized neural circuits. However, it is crucial to note that these enhancements represent potential cognitive improvements, not guaranteed changes. Future research incorporating tests like the California Verbal Learning Test (CVLT), Rey-Osterrieth Complex Figure Test, and the Logical Memory subtest (Wechsler Memory Scale) would be essential to directly investigate the relationship between am-tPCS-induced activation changes and specific memory benefits.

Regarding interhemispheric coherence, promising voxel expansions were observed in medial temporal lobe structures like the hippocampus, parahippocampal gyrus, and amygdala. These areas are crucial for memory formation and consolidation [66]. The 10% bilateral uptick in hippocampal voxels suggests potential synaptic remodeling and a reversal of the atrophy often associated with Alzheimer's pathology [66]. Adjacent parahippocampal areas, including entorhinal regions that represent early disease targets, also exhibited volumetric growth up to 10% (Figures 3 and 4). These changes hint at modified connectivity and plasticity within particularly vulnerable memory structures. Future studies incorporating assessments like the California Verbal Learning Test (CVLT), or Logical Memory (Wechsler Memory Scale) are paramount. These tools directly measure hippocampus-dependent memory function and are vital for determining if increased activation in the hippocampal-parahippocampal circuit offers patients tangible improvements in encoding and recall [67]. This could help prolong memory capacity and delay the onset of significant impairment. Furthermore, boosted amygdala volume potentially aids in stabilizing emotional regulation [68]. Together, these hippocampal modifications, alongside their positive impacts on broader domains like language and visuospatial processing [67], offer early signals that am-tPCS could slow down symptom progression in regions showing Alzheimer's neuropathology [69].

While the observed temporal lobe alterations hint at possible cognitive benefits, it remains uncertain whether interhemispheric coherence voxel changes directly enhance faculties like memory encoding and retrieval. As the hub of semantic and episodic memory networks, determining if heightened temporal metabolism improves real-world functions frequently impaired in Alzheimer's disease requires specific neuropsychological testing. For instance, incorporating delayed recall paradigms could help establish whether improved anterograde memory enables better retention of new verbal or visual information. Equally important are assessments of retrograde semantic and autobiographical memory to clarify if gains in temporal processing mitigate the progressive loss of established memories, impacting activities like conversing, reading comprehension, and navigation. If realized, preserving linguistic and memory capacities would enhance patient independence and quality of life. However, unambiguously linking voxel changes to temporal functions depends on rigorous behavioral outcomes using appropriate neurocognitive measures. Tying metabolic alterations to scores on validated memory batteries would strengthen claims of cognitive benefits stemming from



temporal modulation. In summary, while increased voxel counts hint at plasticity, verifying functional gains remains vital for determining clinical utility.

An in-depth analysis of the temporal lobe demonstrated significant increases in multivariate correlation (MCOR) across critical regions. Remarkably, the left hippocampus displayed a 200% voxel increase (1 to 3 voxels), indicating potentially robust strengthening of medial temporal networks vital for episodic memory and emotional processing. Related parahippocampal and fusiform regions also exhibited marked voxel growth, aligning with their known anatomical connections. Furthermore, average subcortical MCOR counts increased by 120% (0.13 to 0.29 voxels), suggesting even greater signaling capacity in core memory structures. Importantly, a network-level evaluation revealed pronounced improvements in interhemispheric coordination. Sensorimotor areas like the precentral gyrus and central opercular cortex showed striking left-dominant voxel ratios ranging from 1.4 to 2.5 times greater increases (Figures 5 and 6). This asymmetrical pattern hints at the possibility of preferential enhancement in speech production regions within the language-specialized left hemisphere. Collectively, these noteworthy gains in both local temporal circuits and broader inter-network communication provide tantalizing evidence of an overall boost in remaining neural pathways. This could potentially support episodic memory functions and assist in stabilizing emotional regulation – processes often severely compromised in Alzheimer's disease.

Subcortical

A detailed examination of subcortical areas revealed bilateral increases in the voxel and ILC metrics within sensorimotor regions. These findings suggest a potential reactivation and enhancement of residual pathways that could lead to improvements in motor functioning. Notably, the putamen demonstrated bilateral voxel increases across a range of 373% to 571%. This increased activation pattern points to a re-engagement of networks crucial for motor learning and control [70]. Similarly, the pallidum exhibited bilateral voxel spikes of 500-567%, hinting at a potential reintegration of subcortical relays involved in procedural memory. Increased bilateral thalamic voxel counts reaching up to 331% were also observed, potentially reflecting augmented subcortical connectivity, and enhanced signaling patterns, which are often diminished in Alzheimer's Disease and support cortical functions. The amygdala demonstrated considerable bilateral voxel increases of up to 183%, indicating a modulation of pathways influencing socioemotional perception, analysis, and memory capacities via enhanced limbic engagement [71]. Finally, the cerebellum and vermis experienced noticeable increases in ILC metrics. Cerebellar regions displayed increases as high as 47%, whereas the vermis showed ILC increases up to 23% (Figures 1 and 2). These changes suggest improvements in balance, gait, and coordination

While these findings point toward the exciting potential of am-tPCS to positively impact the subcortical networks affected by Alzheimer's disease, further investigations are crucial to solidify these results and establish their clinical significance. Future studies would benefit from directly incorporating targeted assessments to measure actual clinical benefits. For motor outcomes, assessments such as the Timed Up and Go (TUG), Berg Balance Scale, and Purdue Pegboard Test would provide evidence of functional changes. To study potential socioemotional impacts, Facial Emotion Recognition Tests and the Geriatric Depression Scale (GDS) could provide meaningful measurements. An in-depth analysis will unveil the precise mechanisms driving these subcortical modulations and clarify how to promote durable changes through optimized am-tPCS protocols.



Finally, strategic areas like the dorsal striatum, cerebellum, and brain stem displayed considerable interhemispheric coherence activation changes. As crucial modulators of movement, balance, arousal, learning, and overall cognition, determining whether changes in these structures impact function holds promise. For instance, the ~10% uptick in cerebellar voxels hints at amplified integration, which could bolster deteriorating motor control and coordination. Similarly, specialized caudate nucleus changes suggest certain circuitry specific to each hemisphere were selectively targeted (Figures 3 and 4). If proven, this hemispheric calibration could aid failing networks that facilitate planning and inhibition.

Overall, am-tPCS treatment seems to potentially increase activity in networks involved in vital cognitive, behavioral, and physiological processes disrupted by Alzheimer's pathology. The observed structural changes could suggest neuronal remodeling and plasticity, which may reflect an attempt to mitigate the effects of the disease on critical circuits. Future studies incorporating targeted motor evaluations, cognitive assessments, and neurological measures would be essential to verify whether these brain activation changes have true, observable benefits for patients. If findings are consistent and linked to functional improvements, they offer exciting possibilities for developing structural biomarkers and potential therapeutic targets for Alzheimer's interventions. These advances could pave the way for preserving a high quality of life and independence for patients.

Functional Regional + Network Analysis

- **Full Technical Definition**

Alzheimer's disease is associated with disruptions in various large-scale networks, including the Default Mode Network (DMN), Executive Control Network, Salience Network, and Visual Network [72]. So, we decided to explore the large-scale brain network functional connectivity of Alzheimer's disease patients pre- and post-stimulation. In the context of our study, threshold-free cluster enhancement (TFCE) with family-wise error (FWE) correction emerges as an ideal choice for analyzing large-scale brain network connectivity [73]. Traditional statistical methods that rely on arbitrary thresholding or voxel-wise corrections may not be well-suited for large-scale analyses, as they might miss subtle but widespread connectivity patterns or lead to an increased risk of false positives due to multiple comparisons [74]. However, using TFCE-FWE ($p < 0.05$) provides a balanced approach for large-scale functional connectivity analysis, as it leverages the strengths of TFCE for detecting spatially extended patterns while ensuring statistical validity through FWE correction. First, we performed the analysis of the large-scale brain network functional connectivity at baseline (Figure 7). Here are the implications of the analysis pre-stimulation and we will discuss how strengthening this connection could potentially improve the quality of life in patients with Alzheimer's disease.

The baseline connectivity patterns observed in the pre-stimulation phase provide valuable insights into the functional relationships between key brain regions in Alzheimer's patients. The connection between the right superior frontal gyrus (SFG R) and the right posterior parietal cortex (PPC R) suggests active engagement in cognitive processes. This connectivity may be associated with attention, working memory, and executive functions, which are often impaired in Alzheimer's patients. Strengthening this connection through stimulation could potentially lead to improvements in cognitive control and spatial awareness.

Another significant baseline connection is observed between the right frontal pole (FP R) and the right lateral prefrontal cortex (LPFC R). This connection indicates close interaction in executive functions pre-stimulation. Enhancing this connection is



particularly relevant for Alzheimer's patients, as it may improve decision-making and goal-directed behavior, areas frequently impaired in the disease.

Additionally, the baseline connection between the right frontal pole (FP R) and the right angular gyrus (AG R) may have important implications for language and memory functions. Strengthening this connection through stimulation could potentially aid in language comprehension and memory retrieval in Alzheimer's patients, addressing key cognitive deficits associated with the disease [75]. These baseline connectivity patterns provide a foundation for understanding the potential effects of stimulation on brain function in Alzheimer's disease.

Figure 7. Pre + Figure 8. Post

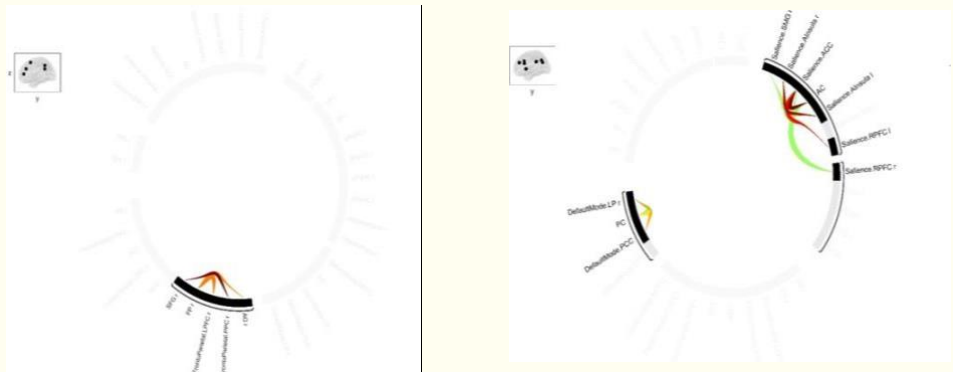


Figure 7 illustrates the large-scale brain network functional connectivity in Alzheimer's disease patients before and after the am-tPCS intervention across 12 weeks. The image shows the connections between key brain regions, with the thickness of the lines representing the strength of the functional connectivity.

Following the stimulation, a striking shift in brain connectivity patterns is evident when comparing the pre-stimulation and post-stimulation data (Figures 8 & 9). Notably, cluster-level changes are observed, with distinct alterations in the TFCE values for clusters 1/1, 1/3, 2/3, and 3/3 post-stimulation, reflecting an impact on the network organization within these clusters (Table 3) [77]. Furthermore, numerous connections exhibit substantial modifications in strength post-stimulation, involving key brain regions such as the anterior cingulate gyrus (ACC), insular cortex (AInsula), supramarginal gyrus (SMG), rostralateral prefrontal cortex (RPF), and lateral parietal cortex (LP) as identified by the Conn Toolbox. These changes are supported by significantly lower p-values and FDR-corrected p-values post-stimulation, underscoring the heightened statistical significance of the post-stimulation results. (Table 3)

Figure 9. Pre and +Figure 10. Post

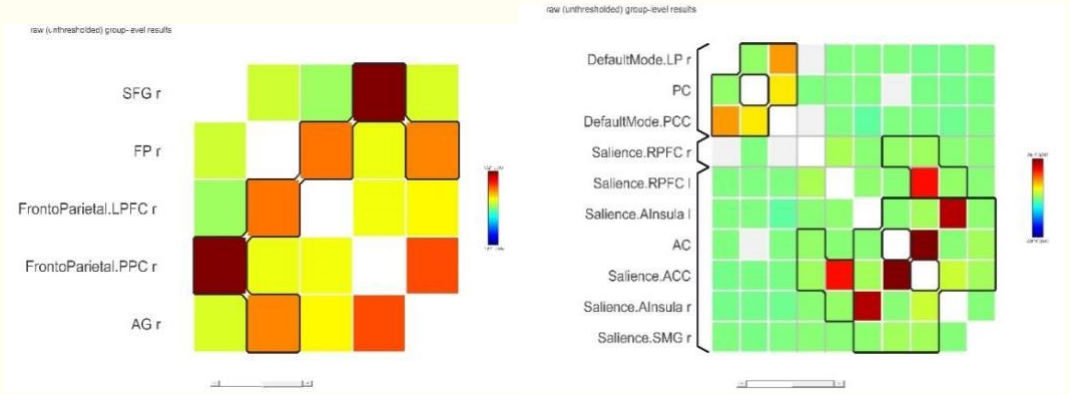


Figure 11. Pre Figure 12. Post

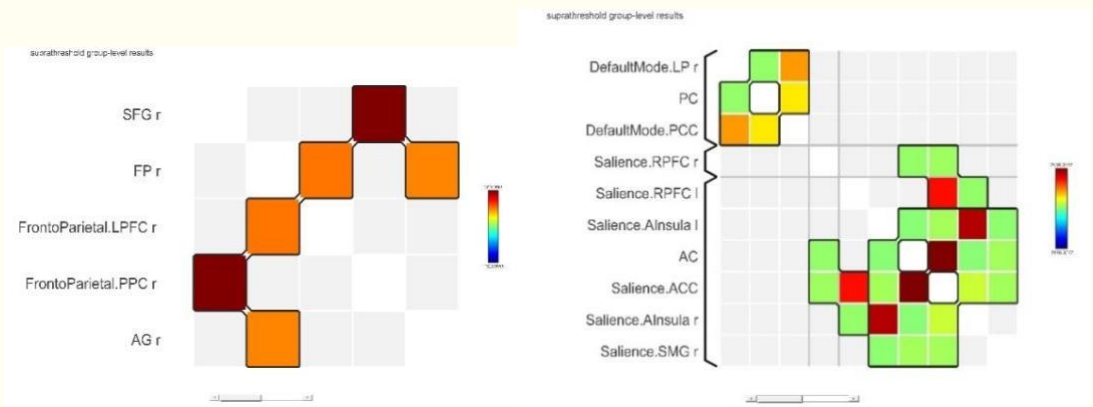


Figure 9+10 and Figure 11+12 display large-scale brain network functional connectivity results in Alzheimer's disease patients before and after a 12-week amplitude-modulated transcranial pulsed current stimulation (am-tPCS) intervention.

In the pre-stimulation phase, notable connections are observed between the right superior frontal gyrus (SFG r) and the right posterior parietal cortex (PPC), the right frontal pole (FP r), and the right lateral prefrontal cortex (LPFC), as well as the right frontal pole and right angular gyrus (AG r).

The post-stimulation phase reveals a striking shift in connectivity patterns compared to pre-stimulation. Several key regions, such as the anterior cingulate gyrus (AC), anterior insula (AInsula), supramarginal gyrus (SMG), rostromedial prefrontal cortex (RPMFC), and lateral parietal cortex (LP), exhibit substantial changes in connection strength.

Table 3: Statistical Significant Clusters

Analysis Unit	Statistic	p-unc	p-FDR	p-FWE
---------------	-----------	-------	-------	-------

Cluster 1/1	TFCE = 1322.00	0.000505	0.015738	0.042000
Connection atlas.SFG r (Superior Frontal Gyrus Right)-networks.FrontoParietal.PPC (R) (52,-52,45)	T(4) = 14.07	0.000148	0.032418	
Connection atlas.FP r (Frontal Pole Right) networks.FrontoParietal.LPFC (R) (41,38,30)	T(4) = 9.52	0.000678	0.040361	
Connection atlas.FP r (Frontal Pole Right) atlas.AG r (Angular Gyrus Right)	T(4) = 9.18	0.000782	0.042276	

Cluster 1/3	TFCE = 2916.35	0.000114	0.008304	0.010000
Connection atlas.AC (Cingulate Gyrus, anterior division)-networks.Saliency.ACC (0,22,35)	T(4) = 18.34	0.000052	0.012803	
Connection networks.Saliency.AInsula (L) (-44,13,1)-networks.Saliency.AInsula (R) (47,14,0)	T(4) = 17.36	0.000065	0.012803	
Connection networks.Saliency.ACC (0,22,35) networks.Saliency.AInsula (R) (47,14,0)	T(4) = 8.32	0.001142	0.051960	
Connection networks.Saliency.AInsula (L) (44,13,1)-networks.Saliency.ACC (0,22,35)	T(4) = 6.09	0.003685	0.068492	
Connection networks.Saliency.ACC (0,22,35) networks.Saliency.SMG (R) (62,-35,32)	T(4) = 6.07	0.003724	0.068492	
Connection atlas.AC (Cingulate Gyrus, anterior division)-networks.Saliency.SMG (R) (62,-35,32)	T(4) = 5.94	0.004031	0.070539	
Connection networks.Saliency.AInsula (L) (-44,13,1)-networks.Saliency.SMG (R) (62,-35,32)	T(4) = 3.68	0.021269	0.147149	
Connection atlas.AC (Cingulate Gyrus, anterior division)-networks.Saliency.AInsula (R) (47,14,0)	T(4) = 3.37	0.028058	0.179512	
Connection networks.Saliency.AInsula (L) (44,13,1)-atlas.AC (Cingulate Gyrus, anterior division)	T(4) = 2.74	0.052064	0.210735	
Cluster 2/3	TFCE = 2112.02	0.000210	0.008304	0.015000
Connection networks.Saliency.RPFC (L) (-32,45,27)-networks.Saliency.ACC (0,22,35)	T(4) = 18.24	0.000053	0.012803	
Connection networks.Saliency.RPFC (R) (32,46,27)-networks.Saliency.ACC (0,22,35)	T(4) = 6.21	0.003430	0.068492	
Connection networks.Saliency.RPFC (R) (32,46,27)-atlas.AC (Cingulate Gyrus, anterior division)	T(4) = 4.81	0.008617	0.088394	



Connection networks.Saliency.RPFC (L) (-32,45,27)-networks.Saliency.AInsula (R) (47,14,0)	T(4) = 4.33	0.012394	0.106877	
Cluster 3/3	TFCE = 1288.78	0.000535	0.013582	0.041000
Connection networks.DefaultMode.LP (R) (47,67,29)-networks.DefaultMode.PCC (1,-61,38)	T(4) = 14.45	0.000133	0.019847	
Connection atlas.PC (Cingulate Gyrus, posterior division)-networks.DefaultMode.PCC (1,-61,38)	T(4) = 11.86	0.000290	0.028743	
Connection networks.DefaultMode.LP (R) (47,67,29)-atlas.PC (Cingulate Gyrus, posterior division)	T(4) = 4.64	0.009734	0.091936	

This finding is particularly promising as it indicates that the stimulation did have a positive impact on brain network connectivity in individuals with Alzheimer's Disease. Increased connectivity in the brain is often associated with improved cognitive function, which is a critical aspect of Alzheimer's disease management. While further research is necessary to fully understand the underlying mechanisms and to establish the long-term effects of this increased connectivity, these initial results are encouraging. They indicate that this intervention may hold potential as a therapeutic approach for enhancing neural connectivity and potentially mitigating the cognitive decline associated with Alzheimer's disease.

The observed changes in functional connectivity between specific brain regions pre- and post-stimulation within the context of Alzheimer's disease may result from the stimulation's impact on neural plasticity and network dynamics. These potential improvements can be explained through various mechanisms and their possible effects on cognitive and emotional functions.

One key area that may show improvement is emotional regulation. The strengthened connection between the left and right anterior insula (AInsula) post-stimulation could indicate improved integration of sensory and emotional information. This enhancement may lead to better emotional regulation and social cognition, which are often affected in Alzheimer's. Similarly, the heightened connectivity between the anterior cingulate gyrus (AC) and the anterior cingulate cortex (ACC) suggests that the intervention might have enhanced the coordination of these regions. Given the ACC's role in emotional regulation and the AC's involvement in cognitive control, this potential improvement may lead to better emotional regulation and possibly help manage mood disturbances frequently seen in Alzheimer's. The enhanced connection between the ACC and the right anterior insula (R-AInsula) post-stimulation could further support emotional regulation and cognitive control [77].

Cognitive control and spatial awareness may also show improvement, as suggested by the strengthened connection between the right superior frontal gyrus (SFG R) and the right posterior parietal cortex (PPC R). This enhanced coordination in brain regions responsible for attention and spatial awareness could potentially lead to improved cognitive control and a better understanding of spatial relationships, possibly ameliorating deficits commonly seen in Alzheimer's patients (Figures 9 and 10).

The stimulation might have promoted neural resilience, potentially allowing regions like the right frontal pole (FP R) and the right angular gyrus (AG R) to better withstand the pathological changes associated with Alzheimer's. This possible resilience



could manifest as improved cognitive functions, such as decision-making and memory retrieval. Additionally, the observed changes may reflect a reorganization of functional brain networks, with the intervention potentially encouraging the brain to establish alternative pathways to compensate for damaged ones. In the context of Alzheimer's, this reorganization could lead to the recruitment of healthier brain regions to perform cognitive and emotional functions, thereby possibly mitigating deficits (Figures 11 and 12).

Social cognition may also benefit from the strengthened connection between the left and right anterior insula (AInsula). This potential improvement in the integration of sensory and emotional information may result in enhanced empathy and emotional understanding, possibly positively impacting social interactions and the overall well-being of Alzheimer's disease patients [77]. The enhanced connection between the ACC and the R-AInsula could contribute to improved emotional control and cognitive flexibility, potentially helping to manage the emotional changes and rigidity in thinking often observed in Alzheimer's patients [77].

Executive functions may see improvement due to the robust connection between the right frontal pole (FP R) and the right lateral prefrontal cortex (LPFC R). This potentially more efficient communication pathway in the brain's executive control network may facilitate better decision-making, planning, and goal-directed behavior, possibly addressing executive function deficits often observed in Alzheimer's disease [87]. Lastly, the connection between FP R and the right angular gyrus (AG R) implies potential benefits for language comprehension and memory retrieval. Strengthening this connection may lead to improved language abilities and better access to stored memories, potentially contributing to enhanced cognitive function in Alzheimer's patients [87].

These findings, as illustrated in Figures 13 and 14, demonstrate the potential of am-tPCS to modulate brain connectivity patterns in Alzheimer's disease, offering promising avenues for therapeutic interventions that may improve cognitive and emotional functions in affected individuals. However, further research is needed to confirm these potential improvements and their clinical significance.

2. Conclusion

Overall, these differences suggest that the stimulation intervention has led to significant changes in brain connectivity patterns. The observed increase in large-scale brain network connectivity during the post-intervention phase suggests that the neurostimulation intervention had a positive impact on the AD brain's functional organization (Figure 10 & 11). The strengthened connections between key brain regions implicated in cognitive and emotional processing may indicate improved information transfer and enhanced integration of neural processes. This finding aligns with the hypothesized therapeutic effects of neurostimulation in Alzheimer's disease.

Figure 13. Pre

+

Figure 14. Post



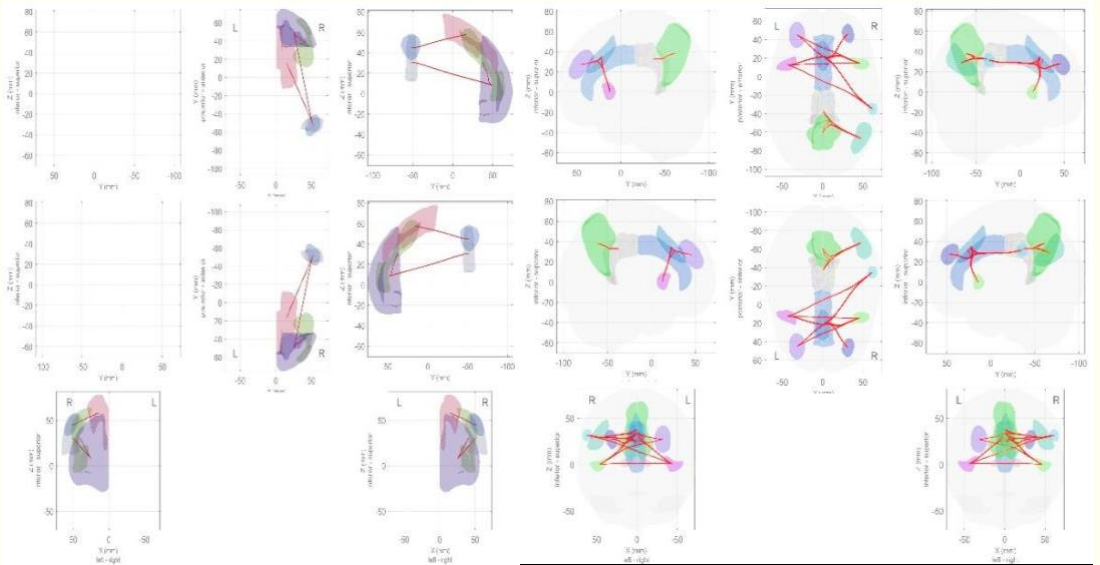


Figure 13 and Figure 14 present brain connectivity patterns in Alzheimer's disease patients before and after a 12-week amplitude-modulated transcranial pulsed current stimulation (am-tPCS) intervention. In these figures, distinct colors are used to represent specific brain regions and their connections. Each color corresponds to a particular area, such as the superior frontal gyrus (SFG), frontal pole (FP), angular gyrus (AG), and various parietal and frontal regions. The presence of a colored line between two brain regions indicates a functional connection, while the absence of a line suggests no significant connection.

3. Future Research

Recent findings suggest that am-tPCS (amplitude-modulated transcranial pulsed current stimulation) has potential for improving cognitive and emotional functions in individuals with Alzheimer's disease. However, as outlined in Table 4 of the original study, current research is limited by several key factors. These limitations include small sample sizes (only 5 participants in the current study), lack of control groups, and fixed stimulation durations of 20 minutes. To address these limitations and fully understand the efficacy of am-tPCS, future studies must employ larger, more diverse sample sizes and conduct long-term follow-up scans at intervals of 1 month, 6 months, and 1 year. Additionally, incorporating detailed neuropsychological evaluations and assessing real-world functional outcomes will provide a more comprehensive understanding of the treatment's impact on patients' lives.

To advance the field, several key studies are proposed. A dose-response trial could help refine optimal stimulation protocols, potentially leading to personalized treatment approaches. A 5-year longitudinal network mapping study, coupled with regular cognitive evaluations, could reveal individual responder profiles and long-term clinical outcomes. Furthermore, a combined intervention trial comparing am-tPCS alone to a multimodal approach with computerized cognitive training could uncover potential synergies and explore treatment sequencing effects.

Future research should also implement more sophisticated statistical techniques, increase sample sizes through multi-site collaborations, and investigate potential

biomarkers to predict treatment response. It's crucial to examine the effectiveness of am-tPCS at different stages of Alzheimer's disease and explore its potential as a preventive measure in high-risk individuals. As research progresses, ethical implications must be considered, ensuring patient safety and well-being remain paramount.

By addressing the limitations outlined in Table 5 and pursuing well-designed future trials, researchers aim to elucidate the full potential of am-tPCS as a therapeutic approach for preserving cognitive function, independence, and quality of life in Alzheimer's disease patients. This ongoing refinement and optimization of am-tPCS protocols may offer new hope to millions affected by this devastating condition, potentially altering its course and improving outcomes for patients and their families.

Funding

This work was supported by U: The Mind Company, a private LLC stationed in Cleveland, Ohio.

Table 4: Limitations	
Limitation	Description
Small Sample Size	The study's primary limitation stems from its notably small sample size, comprising only 5 participants. This diminutive sample raises challenges in generalizing the findings to broader populations. Future studies should prioritize a larger sample to enhance statistical power and establish the consistency of observed effects.
Lack of Control Group	Another critical aspect lacking in the study design is the absence of a control group undergoing a sham procedure or receiving no stimulation. Incorporating a control group would have bolstered the study's validity, enabling more robust claims about the effects attributed specifically to the stimulation intervention.
Fixed Duration of Stimulation	The study administered stimulation for a fixed duration of 20 minutes daily. However, the optimal duration for inducing lasting effects on brain connectivity patterns remains uncertain. Future investigations should explore stimulation durations ranging from 10 to 60 minutes to better understand the nuanced impacts on neural connectivity.
Limited Follow-Up	The study's temporal scope is confined to the immediate post-stimulation period, lacking insights into the long-term maintenance of observed connectivity and network changes. Longitudinal follow-up scans at intervals such as 1 month, 6 months, and 1 year later are imperative to ascertain the enduring effects of am-tPCS modulation.



No Cognitive Assessment	Notably, the study falls short in conducting detailed neuropsychological evaluations to assess real-world impacts of enhanced connectivity. The absence of assessments like MoCA, CANTAB, or MMSE hinders the mapping of cognitive improvements. Comprehensive cognitive profiling is indispensable to elucidate whether enhanced connectivity translates into measurable preservation of memory, attention, and reasoning capacities, thereby potentially prolonging independence in individuals with Alzheimer's disease.
General Lack of Sophistication	A limitation of this study is the reliance on basic statistical analyses. More advanced techniques could potentially reveal additional insights and relationships within the data. We must utilize more sophisticated statistical techniques, such as multilevel modeling to account for nested data structures, Bayesian statistics for incorporating prior knowledge, or causal inference methods to explore potential causal relationships.
Specific Concern about Power	The study may be underpowered to detect smaller effects due to sample size constraints. Future research with a larger sample would increase the statistical power and ability to detect subtler findings. To address this, we must increase sample size in subsequent studies through strategic recruitment efforts, multi-site collaborations, or by leveraging open-access datasets that align with your research question.
Need for Validation of the Chosen Models	The statistical models used in this study have certain assumptions. Future analyses could address those assumptions to establish whether the chosen model selection was optimal, further strengthening the reliability of our findings. Our future action is to carefully assess the assumptions of selected models (e.g., normality, independence of observations) and employ
Limitation	Description
	diagnostic tests to validate their appropriateness. Consider non-parametric or robust statistical methods if assumptions are violated.
Concerns with Multiple Comparisons	Due to the number of comparisons performed, there is a risk of increased false positives (Type I error). In the future, corrections for multiple comparisons should be implemented to limit this risk and enhance the validity of results. In the future, we aim to implement a rigorous correction for multiple comparisons, such as the Bonferroni correction or False Discovery Rate (FDR) methods, to ensure reported findings are robust.

References

1. Marasco, R. A. (2020). Economic burden of Alzheimer's disease and managed care considerations. *The American Journal of Managed Care*, 26(8 Suppl).
2. Morris, K., Nami, M., Bolanos, J. F., Lobo, M. A., Sadri-Naini, M., Fiallos, J., Sanchez, G. E., Bustos, T., Chintam, N., Amaya, M., Strand, S. E., Mayuku-Dore, A., Sakibova, I., Biso, G. M. N., DeFilippis, A., Bravo,



D., Tarhan, N., Claussen, C., Mercado, A., Braun, S., ... Kateb, B. (2021). Neuroscience20 (BRAIN20, SPINE20, and MENTAL20) Health Initiative: A Global Consortium Addressing the Human and Economic Burden of Brain, Spine, and Mental Disorders Through Neurotech Innovations and Policies. *Journal of Alzheimer's disease : JAD*, 83(4), 1563–1601.

3. Nandi, A., Counts, N., Chen, S., Seligman, B., Tortorice, D., Vigo, D., & Bloom, D. E. (2022). Global and regional projections of the economic burden of Alzheimer's disease and related dementias from 2019 to 2050: A value of statistical life approach. *EClinicalMedicine*, 51, 101580.

4. Wong W. (2020). Economic burden of Alzheimer's disease and managed care considerations. *The American journal of managed care*, 26(8 Suppl), S177–S183.

5. Wancata, J., Musalek, M., Alexandrowicz, R., & Krautgartner, M. (2003). Number of dementia sufferers in Europe between the years 2000 and 2050. *European Psychiatry*, 18(6).

6. Di Santo, S. G., Prinelli, F., Adorni, F., Caltagirone, C., & Musicco, M. (2013). A meta-analysis of the efficacy of donepezil, rivastigmine, galantamine, and memantine about the severity of Alzheimer's disease. *Journal of Alzheimer's Disease*, 35(2).

7. Buss, S. S., Fried, P. J., & Pascual-Leone, A. (2019). Therapeutic noninvasive brain stimulation in Alzheimer's disease and related dementias. *Current Opinion in Neurology*, 32(2).

8. Elder, G. J., & Taylor, J. P. (2014). Transcranial magnetic stimulation and transcranial direct current stimulation: Treatments for cognitive and neuropsychiatric symptoms in the neurodegenerative dementias? *Alzheimer's Research and Therapy*, 6(9).

9. Paulus, W. (2003). Chapter 26 Transcranial direct current stimulation (tDCS). *Supplements to Clinical Neurophysiology*, 56(C).

10. Elyamany, O., Leicht, G., Herrmann, C. S., & Mulert, C. (2021). Transcranial alternating current stimulation (tACS): From basic mechanisms towards first applications in psychiatry. *European Archives of Psychiatry and Clinical Neuroscience*, 271(1).



11. Fertonani, A., Pirulli, C., & Miniussi, C. (2011). Random noise stimulation improves neuroplasticity in perceptual learning. *Journal of Neuroscience*, 31(43).
12. Ding, W., Cao, W., Wang, Y., Sun, Y., Chen, X., Zhou, Y., Xu, Q., & Xu, J. (2015). Altered functional connectivity in patients with subcortical vascular cognitive impairment resting-state functional magnetic resonance imaging study. *PLoS ONE*, 10(9).
13. Jaberzadeh, S., Bastani, A., Zoghi, M., Morgan, P., & Fitzgerald, P. B. (2015). Anodal transcranial pulsed current stimulation: The effects of pulse duration on corticospinal excitability. *PLoS ONE*, 10(7).
14. Dissanayaka, T., Zoghi, M., Farrell, M., Egan, G., & Jaberzadeh, S. (2022). The effects of monophasic anodal transcranial pulsed current stimulation on corticospinal excitability and motor performance in healthy young adults: A randomized double-blinded sham-controlled study. *Brain Connectivity*, 12(3).
15. Mamiya, P. C., Richards, T. L., Coe, B. P., Eichler, E. E., & Kuhl, P. K. (2016). Brain white matter structure and COMT gene are linked to second-language learning in adults. *Proceedings of the National Academy of Sciences of the United States of America*, 113(26).
16. Verhelst, H., Dhollander, T., Gerrits, R., & Vingerhoets, G. (2021). Fiber-specific laterality of white matter in left and right language dominant people. *NeuroImage*, 230.
17. Zhang, Y., Lin, L., Feng, M., Dong, L. Y., Qin, Y., Su, H., Zhou, Z., Dai, H., & Wang, Y. (2022). The mean diffusivity of forceps minor is useful to distinguish amnesic mild cognitive impairment from mild cognitive impairment caused by cerebral small vessel disease. *Frontiers in Human Neuroscience*, 16.
18. World Medical Association, "World Medical Association Declaration of Helsinki. Ethical principles for medical research involving human subjects," *Bull. World Health Organ.*, vol. 79, no. 4, pp. 373-374, 2001.



19. Nieto-Castanon, A. (2020). FMRI minimal preprocessing pipeline. In Handbook of functional connectivity Magnetic Resonance Imaging methods in CONN (pp. 3–16). Hilbert Press.
20. Nieto-Castanon, A. (2020). FMRI denoising pipeline. In Handbook of functional connectivity Magnetic Resonance Imaging methods in CONN (pp. 17–25). Hilbert Press.
21. Andersson, J. L., Hutton, C., Ashburner, J., Turner, R., & Friston, K. J. (2001). Modeling geometric deformations in EPI time series. *Neuroimage*, 13(5), 903-919.
22. Fremont, R., Dworkin, J., Manoochehri, M., Krueger, F., Huey, E., & Grafman, J. (2022). Damage to the dorsolateral prefrontal cortex is associated with repetitive compulsive behaviors in patients with penetrating brain injury. *BMJ Neurology Open*, 4(1).
23. Henson, R. N. A., Buechel, C., Josephs, O., & Friston, K. J. (1999). The slice-timing problem in event-related fMRI. *NeuroImage*, 9, 125.
24. Sladky, R., Friston, K. J., Tröstl, J., Cunnington, R., Moser, E., & Windischberger, C. (2011). Slice-timing effects and their correction in functional MRI. *Neuroimage*, 58(2), 588-594.
25. Power, J. D., Mitra, A., Laumann, T. O., Snyder, A. Z., Schlaggar, B. L., & Petersen, S. E. (2014). Methods to detect, characterize, and remove motion artifacts in resting state fMRI. *Neuroimage*, 84, 320-341.
26. Whitfield-Gabrieli, S., Nieto-Castanon, A., & Ghosh, S. (2011). Artifact detection tools (ART). Cambridge, MA. Release Version, 7(19), 11.
27. Calhoun, V.D., Wager, T.D., Krishnan, A., Rosch, K.S., Seymour, K.E., Nebel, M.B., Mostofsky, S.H., Nyalakanai, P. and Kiehl, K. (2017). The impact of T1 versus EPI spatial normalization templates for fMRI data analyses (Vol. 38, No. 11, pp. 5331-5342).
28. Nieto-Castanon, A. (2020). Cluster-level inferences. In Handbook of functional connectivity Magnetic Resonance Imaging methods in CONN (pp. 83–104). Hilbert Press.



29. Ashburner, J., & Friston, K. J. (2005). Unified segmentation. *Neuroimage*, 26(3), 839-851.
30. Ashburner, J. (2007). A fast diffeomorphic image registration algorithm. *Neuroimage*, 38(1), 95-113.
31. Behzadi, Y., Restom, K., Liao, J., & Liu, T. T. (2007). A component-based noise correction method (CompCor) for BOLD and perfusion-based fMRI. *Neuroimage*, 37(1), 90-101.
32. Chai, X. J., Nieto-Castanon, A., Ongur, D., & Whitfield-Gabrieli, S. (2012). Anticorrelations in resting state networks without global signal regression. *Neuroimage*, 59(2), 1420-1428.
33. Hallquist, M. N., Hwang, K., & Luna, B. (2013). The nuisance of nuisance regression: Spectral misspecification in a common approach to resting-state fMRI preprocessing reintroduces noise and obscures functional connectivity. *Neuroimage*, 82, 208-225.
34. Nieto-Castanon, A., & Whitfield-Gabrieli, S. (2021). CONN functional connectivity toolbox: RRID SCR_009550, release 21. doi:10.56441/hilbertpress.2161.7292.
35. Desikan R.S., Ségonne F., Fischl B., Quinn B.T., Dickerson B.C., Blacker D., Buckner R.L., Dale A.M., Maguire R.P., Hyman B.T., Albert M.S., & Killiany R.J. (2006) An automated labeling system for subdividing the human cerebral cortex on MRI scans into gyral based regions of interest. *Neuroimage* 31(3):968-980
36. Nieto-Castanon, A. (2020). General Linear Model. In *Handbook of functional connectivity Magnetic Resonance Imaging methods in CONN* (pp. 63–82). Hilbert Press.
37. Penny, W. D., Friston, K. J., Ashburner, J. T., Kiebel, S. J., & Nichols, T. E. (Eds.). (2011). *Statistical parametric mapping: The analysis of functional brain images*. Elsevier.



38. Smith, S. M., & Nichols, T. E. (2009). Threshold-free cluster enhancement: Addressing problems of smoothing, threshold dependence and localization in cluster inference. *Neuroimage*, 44(1), 83-98.
39. Nieto-Castanon, A. (2020). Functional Connectivity measures. In *Handbook of functional connectivity Magnetic Resonance Imaging methods in CONN* (pp. 26–62). Hilbert Press.
40. Gorgolewski, K., Storkey, A., Bastin, M., & Pernet, C. (2011). Comparison Between FWE and FDR Corrections for Threshold Free Cluster Enhancement Maps. 17th Annual Meeting of the Organization for Human Brain Mapping.
41. Khatri, U., & Kwon, G. R. (2022). Alzheimer's disease diagnosis and biomarker analysis using resting-state functional MRI functional brain network with multi-measures features and hippocampal subfield and amygdala volume of structural MRI. *Frontiers in Aging Neuroscience*, 14.
42. Gonzalez-Gomez, R., Ibañez, A., & Moguilner, S. (2023). Multiclass characterization of frontotemporal dementia variants via multimodal brain network computational inference. *Network Neuroscience*, 7(1).
43. Sala, A., Lizarraga, A., Ripp, I., Cumming, P., & Yakushev, I. (2022). Static versus functional PET: Making sense of metabolic connectivity. *Cerebral Cortex*, 32(5).
44. Wang, Z., Wang, J., Zhang, H., Mchugh, R., Sun, X., Li, K., & Yang, Q. X. (2015). Interhemispheric functional and structural disconnection in Alzheimer's disease: A combined resting-state fMRI and DTI study. *PLoS ONE*, 10(5).
45. Huang, S. Y., Hsu, J. L., Lin, K. J., Liu, H. L., Wey, S. P., Hsiao, I. T., Weiner, M., Aisen, P., Petersen, R., Jack, C. R., Jagust, W., Trojanowki, J. Q., Toga, A. W., Beckett, L., Green, R. C., Saykin, A. J., Morris, J., Shaw, L. M., Liu, E., ... Raj, B. A. (2018). Characteristic patterns of inter- and intra-hemispheric metabolic connectivity in patients with stable and progressive mild cognitive impairment and Alzheimer's disease. *Scientific Reports*, 8(1).
46. Cheung, E. Y. W., Shea, Y. F., Chiu, P. K. C., Kwan, J. S. K., & Mak, H. K. F. (2021). Diagnostic efficacy of voxel-mirrored homotopic connectivity



in vascular dementia as compared to Alzheimer's related neurodegenerative diseases—A resting-state fMRI study. *Life*, 11(10).

47. Dissanayaka, T., Zoghi, M., Farrell, M., Egan, G., & Jaberzadeh, S. (2022). The effects of monophasic anodal transcranial pulsed current stimulation on corticospinal excitability and motor performance in healthy young adults: A randomized double-blinded sham-controlled study. *Brain Connectivity*, 12(3).
48. Mancuso, L., Costa, T., Nani, A., Manuello, J., Liloia, D., Gelmini, G., Panero, M., Duca, S., & Cauda, F. (2019). The homotopic connectivity of the functional brain: A meta-analytic approach. *Scientific Reports*, 9(1).
49. Huang, S. Y., Hsu, J. L., Lin, K. J., & Hsiao, I. T. (2020). A novel individual metabolic brain network for 18F-FDG PET imaging. *Frontiers in Neuroscience*, 14.
50. Xia, Y., & Li, L. (2019). Matrix graph hypothesis testing and application in brain connectivity alternation detection. *Statistica Sinica*, 29(1).
51. Nguyen, D. T., Ryu, S., Qureshi, M. N. I., Choi, M., Lee, K. H., & Lee, B. (2019). Hybrid multivariate pattern analysis combined with extreme learning machine for Alzheimer's dementia diagnosis using multi-measure rs-fMRI spatial patterns. *PLoS ONE*, 14(2).
52. Khazaee, A., Ebrahimzadeh, A., & Babajani-Feremi, A. (2016). Application of advanced machine learning methods on resting-state fMRI network for identification of mild cognitive impairment and Alzheimer's disease. *Brain Imaging and Behavior*, 10(3).
53. Japee, S., Holiday, K., Satyshur, M. D., Mukai, I., & Ungerleider, L. G. (2015). A role of right middle frontal gyrus in reorienting of attention: A case study. *Frontiers in Systems Neuroscience*, 9(MAR).
54. Boisgueheneuc, F. Du, Levy, R., Volle, E., Seassau, M., Duffau, H., Kinkingnehun, S., Samson, Y., Zhang, S., & Dubois, B. (2006). Functions of the left superior frontal gyrus in humans: A lesion study. *Brain*, 129(12).



55. Hornberger, M., & Bertoux, M. (2015). The right lateral prefrontal cortex - Specificity for inhibition or strategy use? *Brain*, 138(4).
56. Voets, N. L., Adcock, J. E., Flitney, D. E., Behrens, T. E. J., Hart, Y., Stacey, R., Carpenter, K., & Matthews, P. M. (2006). Distinct right frontal lobe activation in language processing following left hemisphere injury. *Brain*, 129(3).
57. Alvarez, J. A., & Emory, E. (2006). Executive function and the frontal lobes: A meta-analytic review. *Neuropsychology Review*, 16(1).
58. Singh, A., Trapp, N. T., De Corte, B., Cao, S., Kingyon, J., Boes, A. D., & Parker, K. L. (2019). Cerebellar Theta frequency transcranial pulsed stimulation increases frontal theta oscillations in patients with schizophrenia. *Cerebellum*, 18(3).
59. Binder, J., Frost, J. A., Hammeke, T. A., Bellgowan, P. S. F., Springer, J. A., Kaufman, J. N., & Possing, E. T. (2000). Human temporal lobe activation by speech and nonspeech sounds. *Cerebral Cortex*, 10(5).
60. Riederer, F., Seiger, R., Lanzenberger, R., Patariaia, E., Kasprian, G., Michels, L., Beiersdorf, J., Kollias, S., Czech, T., Hainfellner, J., & Baumgartner, C. (2020). Voxel-based morphometry—from hype to hope. A study on hippocampal atrophy in mesial temporal lobe epilepsy. *American Journal of Neuroradiology*, 41(6).
61. Deture, M. A., & Dickson, D. W. (2019). The neuropathological diagnosis of Alzheimer's disease. *Molecular Neurodegeneration*, 14(1).
62. Duff, M. C., & Brown-Schmidt, S. (2012). The hippocampus and the flexible use and processing of language. *Frontiers in Human Neuroscience*, MARCH 2012.
63. Rasetti, R., Mattay, V. S., White, M. G., Sambataro, F., Podell, J. E., Zolnick, B., Chen, Q., Berman, K. F., Callicott, J. H., & Weinberger, D. R. (2014). Altered hippocampal-parahippocampal function during stimulus encoding. *JAMA Psychiatry*, 71(3).



64. Meyer-Arndt, L., Kuchling, J., Brasanac, J., Hermann, A., Asseyer, S., Bellmann-Strobl, J., Paul, F., Gold, S. M., & Weygandt, M. (2022). Prefrontal-amygdala emotion regulation and depression in multiple sclerosis. *Brain Communications*, 4(3).
65. Vaughn, K. A., Tamber-Rosenau, B. J., & Hernandez, A. E. (2023). The role of the dorsolateral prefrontal cortex in bilingual language switching and non-linguistic task-switching: Evidence from multi-voxel pattern analysis. *Bilingualism: Language and Cognition*, 1–10.
66. Gonzalez-Gomez, R., Ibañez, A., & Moguilner, S. (2023). Multiclass characterization of frontotemporal dementia variants via multimodal brain network computational inference. *Network Neuroscience*, 7(1).
67. Herbet, G., Maheu, M., Costi, E., Lafargue, G., & Duffau, H. (2016). Mapping neuroplastic potential in brain-damaged patients. *Brain*, 139(3).
68. Arai, N., Lu, M. K., Ugawa, Y., & Ziemann, U. (2012). Effective connectivity between human supplementary motor area and primary motor cortex: A paired-coil TMS study. *Experimental Brain Research*, 220(1).
69. Veldema, J., & Gharabaghi, A. (2022). Non-invasive brain stimulation for improving gait, balance, and lower limbs motor function in stroke. *Journal of NeuroEngineering and Rehabilitation*, 19(1).
70. Saeed, U., Compagnone, J., Aviv, R. I., Strafella, A. P., Black, S. E., Lang, A. E., & Masellis, M. (2017). Imaging biomarkers in Parkinson's disease and Parkinsonian syndromes: Current and emerging concepts. *Translational Neurodegeneration*, 6(1).
71. Cheng, W., Rolls, E. T., Qiu, J., Xie, X., Lyu, W., Li, Y., Huang, C. C., Yang, A. C., Tsai, S. J., Lyu, F., Zhuang, K., Lin, C. P., Xie, P., & Feng, J. (2018). Functional connectivity of the human amygdala in health and depression. *Social Cognitive and Affective Neuroscience*, 13(6).
72. Meng, X., Wu, Y., Liang, Y., Zhang, D., Xu, Z., Yang, X., & Meng, L. (2022). A triple-network dynamic connection study in Alzheimer's disease. *Frontiers in Psychiatry*, 13.



73. Watanabe, H., Bagarinao, E., Maesawa, S., Hara, K., Kawabata, K., Ogura, A., Ohdake, R., Shima, S., Mizutani, Y., Ueda, A., Ito, M., Katsuno, M., & Sobue, G. (2021). Characteristics of neural network changes in normal aging and early dementia. *Frontiers in Aging Neuroscience*, 13.

74. Huang, S. Y., Hsu, J. L., Lin, K. J., Liu, H. L., Wey, S. P., Hsiao, I. T., Weiner, M., Aisen, P., Petersen, R., Jack, C. R., Jagust, W., Trojanowki, J. Q., Toga, A. W., Beckett, L., Green, R. C., Saykin, A. J., Morris, J., Shaw, L. M., Liu, E., ... Raj, B. A. (2018). Characteristic patterns of inter- and intra-hemispheric metabolic connectivity in patients with stable and progressive mild cognitive impairment and Alzheimer's disease. *Scientific Reports*, 8(1).

75. Petit, L., Ali, K. M., Rheault, F., Boré, A., Cremona, S., Corsini, F., De Benedictis, A., Descoteaux, M., & Sarubbo, S. (2023). The structural connectivity of the human angular gyrus is revealed by microdissection and diffusion tractography. *Brain Structure and Function*, 228(1).

76. Silva, P. C. D., De Oliveira, L. L. V., Teixeira, R. L. P., Brito, M. L. D. A., & Filippa, A. R. T. M. (2022). Executive functions in Alzheimer's disease: A systematic review. *Journal of Alzheimer's Disease Reports*, 6(1).

77. Horien, C., Shen, X., Scheinost, D., Constable, R. T., & Hampson, M. (2023). Functional connectivity MR imaging. *Functional Neurology: Principles and Clinical Applications*, Second Edition, 521–541.

